

Entangling cavity-magnon polaritons by interacting with phonons

Xuan Zuo,¹ Zhi-Yuan Fan,¹ Hang Qian,¹ Rui-Chang Shen,¹ and Jie Li^{1,*}

¹*Interdisciplinary Center of Quantum Information, State Key Laboratory of Modern Optical Instrumentation, and Zhejiang Province Key Laboratory of Quantum Technology and Device, School of Physics, Zhejiang University, Hangzhou 310027, China*

We show how to entangle two cavity-magnon polaritons (CMPs) formed by two strongly coupled microwave cavity and magnon modes. This is realized by introducing vibration phonons, via magnetostriction, into the system that are dispersively coupled to the magnon mode. Stationary entanglement between two CMPs can be achieved when they are respectively resonant with the two sidebands of the drive field scattered by the phonons, and when the proportions of the cavity and magnon modes in the two polaritons are appropriately chosen. The entangled CMPs can improve the detection sensitivity in the dark matter search experiments using CMPs, and can also lead to the emission of frequency-entangled microwave photons.

I. INTRODUCTION

Cavity magnonics [1], which studies the interaction between microwave cavity photons and magnons in magnetic materials, e.g., yttrium iron garnet (YIG), has attracted great attention and made significant progress in the past decade. The development of the field has been greatly accelerated since the strong cavity-magnon coupling was experimentally achieved [2–4], as theoretically predicted in Ref. [5], benefiting from many excellent properties of the YIG, such as a high spin density and low dissipation rate. The strong coupling leads to the hybridization of the cavity and magnon modes, forming two cavity-magnon polaritons (CMPs). The two hybridized modes are not entangled due to the linear excitation-exchange (beam-splitter-type) interaction between the cavity and magnon modes [6], as the generation of entanglement typically requires the parametric process, external quantum fields, or other novel entangling mechanisms. This is the fundamental reason why it is difficult to entangle the two CMPs. Although many proposals have been put forward in the field for preparing entangled states [7–38], to date a theory for entangling two CMPs is still lacking.

Here, we offer a route to solve this fundamental problem. We show that by introducing a phonon mode that is *dispersively* coupled to the magnon mode (thus forming the cavity magnomechanical system [6]), the two CMPs can be entangled in a stationary state. The phonon mode is used to introduce the parametric down-conversion (PDC) (state-swap) interaction associated with the lower (higher)-frequency polariton mode. By appropriately adjusting the strengths of the PDC and the state-swap interactions, the two CMPs get entangled via the mediation of phonons. The entanglement is robust against thermal noises and dissipation rates of the three modes.

The paper is structured as follows. In Sec. II, we introduce the model and provide the Hamiltonian and Langevin equations of the system. We further derive the linearized Langevin equations for the quantum fluctuations of the system and show how to obtain the steady-state solutions. In Sec. III, we ex-

plain the underlying mechanism for achieving the steady-state entanglement of the two CMPs and present the main results. We then provide optimal conditions for the entanglement and study the effects of the dissipations and input noises of the system on the entanglement. Finally, we summarize our findings in Sec. IV.

II. THE MODEL

The cavity magnomechanical system consists of microwave cavity photons, magnons, and phonons. The cavity and magnon modes are coupled via the magnetic dipole interaction, and the coupling strength can be much larger than two CMPs. The strong coupling results in the normal-mode splitting, as experimentally observed in the cavity magnonic systems [2–

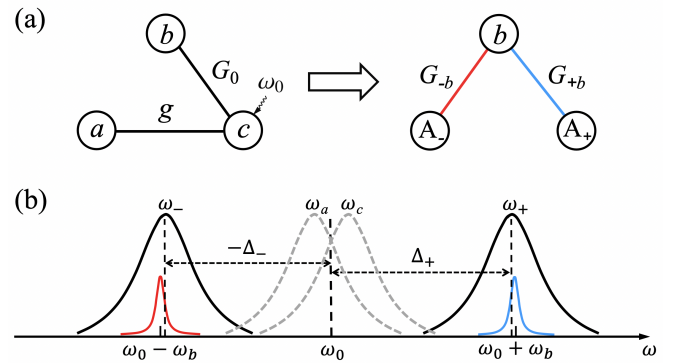


FIG. 1: (a) The cavity magnomechanical system in the strong cavity-magnon coupling regime. The magnon mode c couples to the cavity mode a via a beam-splitter interaction and to the phonon mode b via a dispersive interaction. The cavity and magnon modes are strongly coupled forming two CMP modes A_- and A_+ , of which both are coupled to the phonon mode b . (b) Frequencies and linewidths of the system. The magnon mode c at frequency ω_c is strongly driven by a microwave field at frequency ω_0 , and the phonons at frequency ω_b scatters the driving photons onto the Stokes sideband at $\omega_0 - \omega_b$ and the anti-Stokes sideband at $\omega_0 + \omega_b$. When the frequencies of the two CMPs match the two sidebands, the two CMPs are entangled via the mediation of the phonon mode b .

*jieli007@zju.edu.cn

4]. The magnon mode further dispersively couples to a phonon mode via the magnetostrictive interaction. This is typically the situation where the resonance frequency of the phonon mode is much lower than that of the magnon mode, e.g., for large-size YIG spheres [6]. The system then becomes a hybrid three-mode system, as depicted in Fig. 1(a), with the Hamiltonian given by

$$H/\hbar = \omega_a a^\dagger a + \omega_c c^\dagger c + \omega_b b^\dagger b + G_0 c^\dagger c (b + b^\dagger) + g (a^\dagger c + ac^\dagger) + i\Omega (c^\dagger e^{-i\omega_0 t} - ce^{i\omega_0 t}), \quad (1)$$

where j (j^\dagger), $j = a, c, b$, are the annihilation (creation) operators of the cavity, magnon and phonon modes, respectively, satisfying the commutation relation $[j, j^\dagger] = 1$. ω_j are their corresponding resonance frequencies, and $\omega_b \ll \omega_a, \omega_c$. g denotes the linear cavity-magnon coupling strength, and G_0 is the single-magnon magnomechanical coupling strength. Due to the dispersive nature, G_0 is typically weak, but the effective magnomechanical coupling can be significantly improved by driving the magnon mode with a strong microwave field (at frequency ω_0 and amplitude B_0), and the corresponding Rabi frequency $\Omega = \frac{\sqrt{5}}{4} \gamma_0 \sqrt{N} B_0$ [7], where $\gamma_0/2\pi = 28 \text{ GHz T}^{-1}$ is the gyromagnetic ratio and $N = \rho V$ is the total number of spins, with $\rho = 4.22 \times 10^{27} \text{ m}^{-3}$ being the spin density of the YIG and V as the volume of the YIG sphere.

Since the strongly coupled cavity and magnon modes are hybridized, it is more convenient to describe the cavity-magnon system with two polariton operators A_\pm . The Hamiltonian (1) can then be rewritten in terms of A_\pm and, in the interaction picture with respect to $\hbar\omega_0(A_+^\dagger A_+ + A_-^\dagger A_-)$, is given by (Appendix A)

$$H/\hbar = \Delta_+ A_+^\dagger A_+ + \Delta_- A_-^\dagger A_- + \omega_b b^\dagger b + G_0 (b + b^\dagger) \times \left[A_+^\dagger A_+ \sin^2 \theta + A_-^\dagger A_- \cos^2 \theta + \frac{1}{2} (A_+^\dagger A_- + A_-^\dagger A_+) \sin 2\theta \right] + i\Omega (A_+^\dagger \sin \theta + A_-^\dagger \cos \theta - A_+ \sin \theta - A_- \cos \theta), \quad (2)$$

where A_+ and A_- are the annihilation operators of the two CMPs, which are the hybridization of the cavity and magnon modes via $A_+ = a \cos \theta + c \sin \theta$ and $A_- = -a \sin \theta + c \cos \theta$, with $\theta = \frac{1}{2} \arctan \frac{2g}{\omega_a - \omega_c}$. A_\pm satisfy the bosonic commutation relation $[k, k^\dagger] = 1$ ($k = A_\pm$). $\Delta_\pm = \omega_\pm - \omega_0$ denote the polariton-drive detunings, where $\omega_\pm = \frac{1}{2} [\omega_a + \omega_c \pm \sqrt{(\omega_a - \omega_c)^2 + 4g^2}]$ are the frequencies of the two CMPs, cf. Fig. 1(b).

By including the dissipation and input noise of each mode, we obtain the following quantum Langevin equations (QLEs)

of the system (Appendix B):

$$\begin{aligned} \dot{A}_+ &= -i\Delta_+ A_+ - iG_0 (b + b^\dagger) (A_+ \sin^2 \theta + A_- \sin \theta \cos \theta) \\ &\quad - \kappa_+ A_+ - \delta\kappa A_- + \Omega \sin \theta + \sqrt{2\kappa_+} A_+^{in}, \\ \dot{A}_- &= -i\Delta_- A_- - iG_0 (b + b^\dagger) (A_- \cos^2 \theta + A_+ \cos \theta \sin \theta) \\ &\quad - \kappa_- A_- - \delta\kappa A_+ + \Omega \cos \theta + \sqrt{2\kappa_-} A_-^{in}, \\ \dot{b} &= -i\omega_b b - iG_0 (A_+^\dagger A_+ \sin^2 \theta + A_-^\dagger A_- \sin \theta \cos \theta \\ &\quad + A_-^\dagger A_+ \cos \theta \sin \theta + A_-^\dagger A_- \cos^2 \theta) - \kappa_b b + \sqrt{2\kappa_b} b^{in}, \end{aligned} \quad (3)$$

where $\kappa_+ \equiv \kappa_a \cos^2 \theta + \kappa_c \sin^2 \theta$ and $\kappa_- \equiv \kappa_a \sin^2 \theta + \kappa_c \cos^2 \theta$ are the dissipation rates of the two polaritons A_+ and A_- , respectively, and $\delta\kappa \equiv (\kappa_c - \kappa_a) \sin \theta \cos \theta$ denotes the coupling strength between the two CMPs due to the unbalanced dissipation rates $\kappa_a \neq \kappa_c$, with κ_j being the dissipation rate of the mode j ($j = a, c, b$). $A_+^{in} \equiv (\sqrt{2\kappa_a} \cos \theta a^{in} + \sqrt{2\kappa_c} \sin \theta c^{in})/\sqrt{2\kappa_+}$ and $A_-^{in} \equiv (-\sqrt{2\kappa_a} \sin \theta a^{in} + \sqrt{2\kappa_c} \cos \theta c^{in})/\sqrt{2\kappa_-}$ represent the noises entering the two CMPs, which are related to the input noises a^{in} , c^{in} of the original cavity and magnon modes, and b^{in} is the input noise of the phonon mode. The input noises $j^{in}(t)$, $j = a, c, b$, are zero-mean and characterized by the correlation functions [39]: $\langle j^{in}(t) j^{in\dagger}(t') \rangle = [N_j(\omega_j) + 1] \delta(t - t')$, $\langle j^{in\dagger}(t) j^{in}(t') \rangle = N_j(\omega_j) \delta(t - t')$, with $N_j(\omega_j) = [\exp(\hbar\omega_j/k_B T) - 1]^{-1}$ being the equilibrium mean thermal excitation number of the mode j , and T as the bath temperature.

Since the magnon mode is strongly driven and due to its excitation-exchange interaction with the cavity mode, the two CMPs have large amplitudes $|\langle A_+ \rangle|, |\langle A_- \rangle| \gg 1$ at the steady state. This allows us to linearize the nonlinear dispersive interaction around the large average values [7, 40]. This is implemented by writing each mode operator O , $O = A_+, A_-, b$, as the sum of its classical average and quantum fluctuation operator, i.e., $O = \langle O \rangle + \delta O$, and neglecting small second-order fluctuation terms in Eq. (3). We aim to study quantum entanglement between the two CMPs, and hence focus on the dynamics of the quantum fluctuations. The quantum fluctuations of the system ($\delta A_+, \delta A_-, \delta b$) are governed by the following linearized QLEs (Appendix B):

$$\begin{aligned} \delta \dot{A}_+ &= -(i\Delta_+ + \kappa_+) \delta A_+ - \delta\kappa \delta A_- - G_{+b} \frac{\delta b + \delta b^\dagger}{2} + \sqrt{2\kappa_+} A_+^{in}, \\ \delta \dot{A}_- &= -(i\Delta_- + \kappa_-) \delta A_- - \delta\kappa \delta A_+ - G_{-b} \frac{\delta b + \delta b^\dagger}{2} + \sqrt{2\kappa_-} A_-^{in}, \\ \delta \dot{b} &= -(i\omega_b + \kappa_b) \delta b - \left(\frac{G_{+b}}{2} \delta A_+^\dagger + \frac{G_{-b}}{2} \delta A_-^\dagger - \text{H.c.} \right) + \sqrt{2\kappa_b} b^{in}, \end{aligned} \quad (4)$$

where $G_{+b} \equiv G_{+-} \sin \theta$ ($G_{-b} \equiv G_{+-} \cos \theta$) represents the coupling strength between the polariton A_+ (A_-) and the phonon mode b , with $G_{+-} \equiv G_+ \sin \theta + G_- \cos \theta$, and $G_\pm = i2G_0 \langle A_\pm \rangle$ being the enhanced dispersive coupling strengths associated with the two CMPs. In obtaining Eq. (4), we neglect the linear coupling terms between the two CMPs $\mathcal{G}(\delta A_+^\dagger \delta A_- + \delta A_+ \delta A_-^\dagger)$, where $\mathcal{G} = G_0 \text{Re}\langle b \rangle \sin 2\theta$, due to their weak strength and negligible impact on the entanglement. Under the optimal conditions for the entanglement

$|\Delta_{\pm}| \simeq \omega_b \gg \kappa_{\pm}$ (cf. Fig. 1(b)), as will be discussed later, we obtain approximate analytical expressions of the steady-state averages, i.e.,

$$\begin{aligned} \langle A_+ \rangle &\simeq \frac{\delta\kappa\Omega \cos\theta - i\Omega \sin\theta(\Delta_- - i\kappa_-)}{(\Delta_- - i\kappa_-)(\Delta_+ - i\kappa_+) + \delta\kappa^2}, \\ \langle A_- \rangle &\simeq \frac{\delta\kappa\Omega \sin\theta - i\Omega \cos\theta(\Delta_+ - i\kappa_+)}{(\Delta_- - i\kappa_-)(\Delta_+ - i\kappa_+) + \delta\kappa^2}, \\ \text{Re}\langle b \rangle &= -\frac{G_0}{\omega_b} \left[\langle A_+ \rangle \sin\theta + \langle A_- \rangle \cos\theta \right]^2. \end{aligned} \quad (5)$$

Because of the weak coupling G_0 , the frequency shift caused by the dispersive coupling is typically much smaller than the resonance frequency ω_b , as observed in the magnomechanical experiments [41–43]. Therefore, in deriving Eqs. (4) and (5) we safely neglect this small frequency shift in the detunings $|\Delta_{\pm}| \simeq \omega_b$.

The QLEs (4) can be expressed using quadratures $(\delta X_{\pm}, \delta Y_{\pm}, \delta X_b, \delta Y_b)$, with $\delta X_{\pm} = (\delta A_{\pm} + \delta A_{\pm}^{\dagger})/\sqrt{2}$, $\delta Y_{\pm} = i(\delta A_{\pm}^{\dagger} - \delta A_{\pm})/\sqrt{2}$, and $\delta X_b = (\delta b + \delta b^{\dagger})/\sqrt{2}$, $\delta Y_b = i(\delta b^{\dagger} - \delta b)/\sqrt{2}$, and cast in the matrix form of

$$\dot{u}(t) = \mathcal{R}u(t) + n(t), \quad (6)$$

where $u(t) = [\delta X_+(t), \delta Y_+(t), \delta X_-(t), \delta Y_-(t), \delta X_b(t), \delta Y_b(t)]^T$, $n(t) = [\sqrt{2\kappa_+}X_+^{in}, \sqrt{2\kappa_+}Y_+^{in}, \sqrt{2\kappa_-}X_-^{in}, \sqrt{2\kappa_-}Y_-^{in}, \sqrt{2\kappa_b}X_b^{in}, \sqrt{2\kappa_b}Y_b^{in}]^T$, and the drift matrix \mathcal{R} is given by

$$\mathcal{R} = \begin{pmatrix} -\kappa_+ & \Delta_+ & -\delta\kappa & 0 & -\text{Re} G_{+b} & 0 \\ -\Delta_+ & -\kappa_+ & 0 & -\delta\kappa & -\text{Im} G_{+b} & 0 \\ -\delta\kappa & 0 & -\kappa_- & \Delta_- & -\text{Re} G_{-b} & 0 \\ 0 & -\delta\kappa & -\Delta_- & -\kappa_- & -\text{Im} G_{-b} & 0 \\ 0 & 0 & 0 & 0 & -\kappa_b & \omega_b \\ -\text{Im} G_{+b} & \text{Re} G_{+b} & -\text{Im} G_{-b} & \text{Re} G_{-b} & -\omega_b & -\kappa_b \end{pmatrix}. \quad (7)$$

Since the quantum noises are Gaussian and the system dynamics is linearized, the steady state of the quadrature fluctuations is a continuous-variable three-mode Gaussian state, which can be completely characterized by a 6×6 covariance matrix (CM) V with its entries defined as $V_{ij} = \frac{1}{2} \langle u_i(t)u_j(t') + u_j(t')u_i(t) \rangle$ ($i, j = 1, 2, \dots, 6$). The steady-state CM V can be achieved by directly solving the Lyapunov equation [40]

$$\mathcal{R}V + V\mathcal{R}^T = -D, \quad (8)$$

where $D = \text{Diag}[\kappa_+(2N_+ + 1), \kappa_+(2N_+ + 1), \kappa_-(2N_- + 1), \kappa_-(2N_- + 1), \kappa_b(2N_b + 1), \kappa_b(2N_b + 1)] + \frac{1}{2} \tan 2\theta [-\kappa_+(2N_+ + 1) + \kappa_-(2N_- + 1)] \sigma^x \otimes \mathbb{I}_{2 \times 2} \oplus \mathbb{0}_{2 \times 2}$ is the diffusion matrix, which is defined via $D_{ij} \delta(t-t') = \langle n_i(t)n_j(t') + n_j(t')n_i(t) \rangle/2$. σ^x is the x -Pauli matrix and the mean thermal excitation numbers N_{\pm} are related to N_a and N_c via $N_+ = \{[\kappa_a \cos^2 \theta (2N_a + 1) + \kappa_c \sin^2 \theta (2N_c + 1)]/\kappa_+ - 1\}/2$ and $N_- = \{[\kappa_a \sin^2 \theta (2N_a + 1) + \kappa_c \cos^2 \theta (2N_c + 1)]/\kappa_- - 1\}/2$. We adopt the logarithmic negativity E_N [44–46] to quantify the entanglement between the two CMPs, which is defined based on the 4×4 CM V_4 of the two polariton modes (V_4 is extracted by removing irrelevant rows and

columns in V). Specifically, $E_N = \max[0, -\ln(2\eta^-)]$, where $\eta^- \equiv 2^{-1/2} [\Sigma - (\Sigma^2 - 4 \det V_4)^{1/2}]^{1/2}$, and $V_4 = [V_+, V_{+-}; V_{+-}^T, V_-]$, with V_+ , V_- and V_{+-} being the 2×2 blocks of V_4 , and $\Sigma \equiv \det V_+ + \det V_- - 2 \det V_{+-}$.

III. ENTANGLEMENT OF TWO CMPs

The mechanism of creating entanglement between the two CMPs is as follows. The phonons scatter the driving microwave photons at frequency ω_0 onto two sidebands at $\omega_0 \pm \omega_b$ (cf. Fig. 1(b)). When the frequencies of the two CMPs are adjusted to be resonant with the two sidebands, i.e., $\Delta_+ = -\Delta_- \simeq \omega_b$, both the Stokes and anti-Stokes scatterings are effectively activated, where the Stokes scattering corresponds to the PDC interaction causing the lower-frequency polariton to be entangled with the phonon mode, while the anti-Stokes scattering leads to the state-swap (beam-splitter) interaction between the higher-frequency polariton and the phonon mode. Therefore, the two CMPs get entangled via the mediation of phonons when the above two processes are simultaneously activated.

The interactions between the CMPs and the phonon mode essentially result from the dispersive coupling between the phonon mode and the component of the magnon mode in the CMPs. Therefore, by varying the proportion of the magnon mode in the polaritons (via altering θ), one can adjust the *effective* strength of the PDC (state-swap) interaction associated with the Stokes (anti-Stokes) scattering. For the spe-

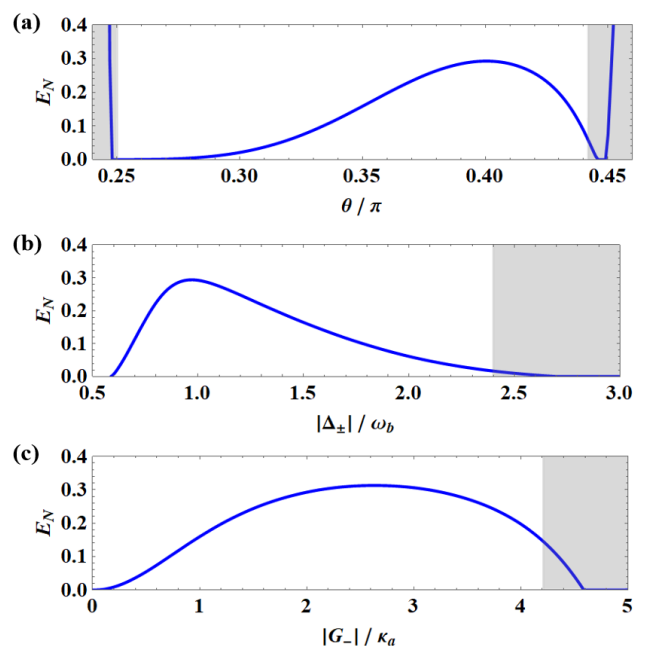


FIG. 2: Stationary entanglement between two CMPs E_N versus (a) θ ; (b) the polariton-drive detuning $|\Delta_{\pm}|$; (c) the coupling strength $|G_-|$. We take $|G_-|/2\pi = 2$ MHz and $\Delta_+ = -\Delta_- = \omega_b$ in (a). The parameters of (b) [(c)], apart from Δ_{\pm} ($|G_-|$), correspond to those yielding an optimal angle $\theta \simeq 0.40\pi$ in (a). The grey areas denote the regimes where the system is unstable. See text for other parameters.

cial case $\theta = \frac{\pi}{4}$, $\theta \in [0, \frac{\pi}{2}]$, where both the CMPs A_{\pm} have equally weighted cavity and magnon modes, the strengths of the Stokes and anti-Stokes scatterings are equal. This point easily causes the system to be unstable (cf. Fig. 2(a)) and only nonstationary entanglement could be produced [47]. Therefore, a larger $\theta > \frac{\pi}{4}$ should be considered to obtain stationary entanglement, where the anti-Stokes scattering (for mechanical cooling) outperforms the Stokes scattering (for mechanical amplification). For a relatively small value of θ , e.g., $\theta < \frac{\pi}{3}$, we find that the entanglement between the two CMPs is small, while the entanglement between the lower-frequency polariton A_- and phonons is strong. This indicates that the entanglement (A_- & b) is effectively generated by the Stokes scattering, but is not yet efficiently transferred to the higher-frequency polariton A_+ . The state-swap interaction between the polariton A_+ and the phonon mode b in the anti-Stokes scattering should thus be enhanced. To this end, we further increase θ to raise the proportion of the magnon mode in the polariton A_+ , which enhances the strength of the anti-Stokes scattering. Consequently, we see an efficient entanglement transfer and the two CMPs are strongly entangled around $\theta \simeq 0.40\pi$, as clearly shown in Fig. 2(a). However, θ cannot be too large (i.e., too close to $\frac{\pi}{2}$), as this reduces the proportion of the magnon mode in the polariton A_- and thus the strength of the associated Stokes scattering, from which the entanglement of the system originates. Therefore, an optimal θ exists for the entanglement as the result of the trade-off between the strengths of the Stokes and anti-Stokes scatterings, as seen in Fig. 2(a).

In Fig. 2, we use experimentally feasible parameters [6]: $\omega_a/2\pi = 10$ GHz, $\omega_b/2\pi = 10$ MHz, $\kappa_a/2\pi = \kappa_c/2\pi = 1$ MHz, $\kappa_b/2\pi = 100$ Hz, and at low temperature $T = 10$ mK. We further consider the optimal detunings $\Delta_+ = -\Delta_- = \omega_b$ in Fig. 2(a), as analyzed above. For a given θ , g and ω_c can be determined by solving the equations $\theta = \frac{1}{2} \arctan \frac{2g}{\omega_a - \omega_c}$ and $\sqrt{(\omega_a - \omega_c)^2 + 4g^2} = 2\omega_b$ ($\omega_{a,b}$ are assumed constant). We note that the magnon frequency ω_c and the cavity-magnon coupling strength g can be readily adjusted, respectively, by varying the bias magnetic field and the position of the YIG sphere inside the microwave cavity [2–4]. The stability of the system is guaranteed by the negative eigenvalues (real parts) of the drift matrix \mathcal{R} . We find that, apart from the unstable region when θ is small ($\theta \leq 0.25\pi$), the system can also be unstable when θ is too large. This is because the coupling strength $|G_+|$ (associated with the polariton A_+) increases rapidly as θ grows, $\theta \rightarrow \frac{\pi}{2}$, due to the relation $|\frac{G_+}{G_-}| \simeq \tan \theta$ ($|G_-|$ is fixed in Fig. 2(a)).

An optimal $\theta \simeq 0.40\pi$ gives the maximum entanglement in Fig. 2(a), which corresponds to $g/2\pi \simeq 5.88$ MHz and $\omega_c/2\pi \simeq 10.0162$ GHz. To investigate the effect of the deviation of the polaritons from the mechanical sidebands, we change ω_c in Fig. 2(b) to vary the polariton frequencies (i.e., Δ_{\pm}). Specifically, we set the drive frequency $\omega_0 = \frac{\omega_a + \omega_c}{2}$, which ensures two symmetric CMPs ($\Delta_+ = |\Delta_-|$) and mechanical sidebands with respect to the drive frequency. It shows that when the two CMPs deviate from the two mechanical sidebands ($|\Delta_{\pm}|$ away from ω_b), the entanglement reduces, confirming our earlier analysis on the optimal condi-

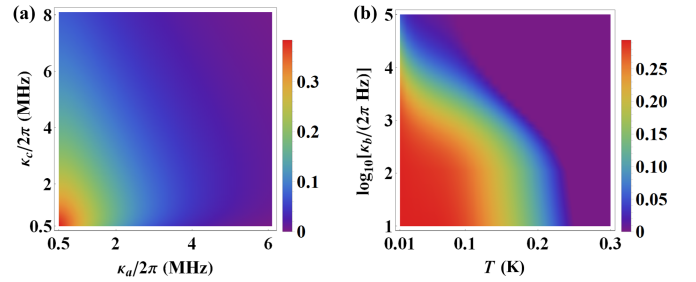


FIG. 3: Stationary polariton entanglement E_N versus (a) dissipation rates κ_a and κ_c ; (b) bath temperature T and κ_b . We take $\theta \simeq 0.40\pi$, and the other parameters are the same as in Fig. 2(a).

tion $\Delta_+ = -\Delta_- \simeq \omega_b$ for the entanglement. The unstable region is because that a large $|\Delta_{\pm}|$ corresponds to θ approaching $\frac{\pi}{2}$, and thus a large value of $|G_+|$. This is similar to the reason of the instability on the right side of Fig. 2(a).

In Fig. 2(c), we plot the entanglement versus the effective coupling rate G_- . Clearly, as $|G_-|$ grows the entanglement reaches its maximum in the stable regime and then reduces before entering the unstable regime. This means that one can obtain the maximum entanglement *in the stable regime*, and the maximum entanglement is no longer constrained by the stability condition [40, 48]. This implies that the entanglement mechanism presented here fundamentally differs from those in the protocols of, e.g., Refs. [7, 40].

It should be noted that the results of Fig. 2 are obtained under the condition of $\kappa_a \simeq \kappa_c$. For the case of $\delta\kappa$ being comparable to or larger than $\kappa_{a(c)}$, the associated coupling terms between the two CMPs (cf. Eq. (4)) may have a significant impact on the entanglement. In Fig. 3(a), we plot the entanglement versus the two dissipation rates κ_a and κ_c . It shows that for a wide range of $\kappa_{a(c)}$, the entanglement is present. The entanglement is also robust with respect to the bath temperature T and the mechanical damping rate κ_b , as shown in Fig. 3(b). The entanglement survives for the temperature up to $T \approx 220$ mK (κ_b up to $\sim 2\pi \times 10^5$ Hz), under experimentally feasible parameters.

IV. CONCLUSION

We present a mechanism of entangling two CMPs in cavity magnonics by dispersively coupling magnons with vibration phonons via introducing magnetostriction. The presence of the vibration phonon mode activates the PDC and the state-swap interactions associated with the two polariton modes, which become entangled when the strengths of the two interactions are properly chosen. The work fills the gap in the study of entangling two CMPs and finds potential applications in the study of macroscopic quantum states and quantum metrology, e.g., it can be applied to improve the detection sensitivity in the dark matter search experiments using CMPs [49–51] by exploiting the entanglement shared between the polaritons [52, 53]. The entangled CMPs can also lead to the emission of frequency-entangled microwave photons [54],

which may find applications in microwave quantum information processing.

ACKNOWLEDGMENTS

This work has been supported by National Key Research and Development Program of China (Grant No. 2022YFA1405200) and National Natural Science Foundation of China (Grant No. 92265202).

APPENDIX A: POLARITON MODES

The Hamiltonian of the cavity and magnon modes with a beam-splitter-type linear coupling reads

$$\begin{aligned} H/\hbar &= \omega_a a^\dagger a + \omega_c c^\dagger c + g(a^\dagger c + ac^\dagger) \\ &= \begin{pmatrix} a^\dagger & c^\dagger \end{pmatrix} \begin{pmatrix} \omega_a & g \\ g & \omega_c \end{pmatrix} \begin{pmatrix} a \\ c \end{pmatrix}, \end{aligned} \quad (\text{A1})$$

where a and c ($[O, O^\dagger] = 1$, $O = a, c$) are the annihilation operators of the cavity and magnon modes with resonance frequencies ω_a and ω_c , and g is the coupling strength. When the two modes are nearly resonant and strongly coupled, $g > \kappa_a, \kappa_c$, with κ_a and κ_c being their dissipation rates, the cavity and magnon modes form two CMPs. By diagonalizing the interaction matrix, we obtain the Hamiltonian of the two CMP modes

$$H/\hbar = \omega_+ A_+^\dagger A_+ + \omega_- A_-^\dagger A_-, \quad (\text{A2})$$

where A_+ and A_- ($[O, O^\dagger] = 1$, $O = A_+, A_-$) denote the two polariton modes, and ω_+ and ω_- are their eigenfrequencies

$$\begin{aligned} \omega_+ &= \frac{\omega_a + \omega_c + \sqrt{(\omega_a - \omega_c)^2 + 4g^2}}{2}, \\ \omega_- &= \frac{\omega_a + \omega_c - \sqrt{(\omega_a - \omega_c)^2 + 4g^2}}{2}. \end{aligned} \quad (\text{A3})$$

Clearly, for the resonant case $\omega_a = \omega_c$, $\omega_+ - \omega_- = 2g$. The two CMP modes A_\pm are the hybridization of the original cavity and magnon modes, reflected in the following transformation matrix

$$\begin{pmatrix} A_+ \\ A_- \end{pmatrix} = \begin{pmatrix} \cos \theta & \sin \theta \\ -\sin \theta & \cos \theta \end{pmatrix} \begin{pmatrix} a \\ c \end{pmatrix}, \quad (\text{A4})$$

where

$$\theta = \frac{1}{2} \arctan \frac{2g}{\omega_a - \omega_c}. \quad (\text{A5})$$

Including vibration phonons, the Hamiltonian of the cavity magnomechanical system under study is given by (i.e., Eq. (1) in the main text)

$$\begin{aligned} H/\hbar &= \omega_a a^\dagger a + \omega_c c^\dagger c + \omega_b b^\dagger b + G_0 c^\dagger c (b + b^\dagger) \\ &+ g(a^\dagger c + ac^\dagger) + i\Omega(c^\dagger e^{-i\omega_0 t} - ce^{i\omega_0 t}). \end{aligned} \quad (\text{A6})$$

For strongly coupled cavity and magnon modes, it is more convenient to describe the system with polariton operators A_\pm . The Hamiltonian (A6) can then be rewritten as

$$\begin{aligned} H/\hbar &= \omega_+ A_+^\dagger A_+ + \omega_- A_-^\dagger A_- + \omega_b b^\dagger b \\ &+ G_0 (b + b^\dagger) (A_+^\dagger A_+ \sin^2 \theta + A_+^\dagger A_- \sin \theta \cos \theta \\ &\quad + A_-^\dagger A_+ \cos \theta \sin \theta + A_-^\dagger A_- \cos^2 \theta) \\ &+ i\Omega (A_+^\dagger \sin \theta e^{-i\omega_0 t} + A_-^\dagger \cos \theta e^{-i\omega_0 t} \\ &\quad - A_+ \sin \theta e^{i\omega_0 t} - A_- \cos \theta e^{i\omega_0 t}). \end{aligned} \quad (\text{A7})$$

Working in the interaction picture with respect to $\hbar\omega_0(A_+^\dagger A_+ + A_-^\dagger A_-)$, the Hamiltonian (A7) becomes in the following form

$$\begin{aligned} H/\hbar &= \Delta_+ A_+^\dagger A_+ + \Delta_- A_-^\dagger A_- + \omega_b b^\dagger b + G_0 (b + b^\dagger) \\ &\times \left[A_+^\dagger A_+ \sin^2 \theta + A_-^\dagger A_- \cos^2 \theta + \frac{1}{2} (A_+^\dagger A_- + A_-^\dagger A_+) \sin 2\theta \right] \\ &+ i\Omega (A_+^\dagger \sin \theta + A_-^\dagger \cos \theta - A_+ \sin \theta - A_- \cos \theta), \end{aligned} \quad (\text{A8})$$

where the polariton-drive detunings $\Delta_\pm = \omega_\pm - \omega_0$.

APPENDIX B: LINEARIZED QUANTUM LANGEVIN EQUATIONS

The Hamiltonian (A6) corresponds to the following quantum Langevin equations (QLEs) by including the dissipation and input noise of each mode:

$$\begin{aligned} \dot{a} &= -(i\Delta_a + \kappa_a)a - igc + \sqrt{2\kappa_a}a^{in}, \\ \dot{c} &= -(i\Delta_c + \kappa_c)c - iga - iG_0c(b + b^\dagger) + \Omega + \sqrt{2\kappa_c}c^{in}, \\ \dot{b} &= -i\omega_b b - iG_0c^\dagger c - \kappa_b b + \sqrt{2\kappa_b}b^{in}, \end{aligned} \quad (\text{B1})$$

where $\Delta_a = \omega_a - \omega_0$, and $\Delta_c = \omega_c - \omega_0$. The above QLEs can be rewritten in terms of polariton operators A_\pm for strongly coupled cavity and magnon modes, given by

$$\begin{aligned} \dot{A}_+ &= -i\Delta_+ A_+ - iG_0 (b + b^\dagger) (A_+ \sin^2 \theta + A_- \sin \theta \cos \theta) \\ &\quad - \kappa_+ A_+ - \delta\kappa A_- + \Omega \sin \theta + \sqrt{2\kappa_+} A_+^{in}, \\ \dot{A}_- &= -i\Delta_- A_- - iG_0 (b + b^\dagger) (A_- \cos^2 \theta + A_+ \cos \theta \sin \theta) \\ &\quad - \kappa_- A_- - \delta\kappa A_+ + \Omega \cos \theta + \sqrt{2\kappa_-} A_-^{in}, \\ \dot{b} &= -i\omega_b b - iG_0 (A_+^\dagger A_+ \sin^2 \theta + A_+^\dagger A_- \sin \theta \cos \theta \\ &\quad + A_-^\dagger A_+ \cos \theta \sin \theta + A_-^\dagger A_- \cos^2 \theta) - \kappa_b b + \sqrt{2\kappa_b} b^{in}, \end{aligned} \quad (\text{B2})$$

where we define $\kappa_+ \equiv \kappa_a \cos^2 \theta + \kappa_c \sin^2 \theta$, $\kappa_- \equiv \kappa_a \sin^2 \theta + \kappa_c \cos^2 \theta$, which can be interpreted as the dissipation rates of the two CMP modes, and $\delta\kappa \equiv (\kappa_c - \kappa_a) \sin \theta \cos \theta$, which denotes the *direct* coupling strength between the two CMPs due to the unbalanced dissipation rates $\kappa_a \neq \kappa_c$. The two CMPs

can also be *indirectly* coupled via the mediation of the phonon mode with the coupling strength of $G_0\text{Re}\langle b \rangle \sin 2\theta \equiv \mathcal{G}$.

Under a strong drive field, the QLEs (B2) can be linearized around large average values. We obtain the following linearized QLEs describing the quantum fluctuations of the system $(\delta A_+, \delta A_-, \delta b)$, which are

$$\begin{aligned}\delta\dot{A}_+ &= -(i\tilde{\Delta}_+ + \kappa_+)\delta A_+ - (i\mathcal{G} + \delta\kappa)\delta A_- - G_{+b}\frac{\delta b + \delta b^\dagger}{2} + \sqrt{2\kappa_+}A_+^{in}, \\ \delta\dot{A}_- &= -(i\tilde{\Delta}_- + \kappa_-)\delta A_- - (i\mathcal{G} + \delta\kappa)\delta A_+ - G_{-b}\frac{\delta b + \delta b^\dagger}{2} + \sqrt{2\kappa_-}A_-^{in}, \\ \delta\dot{b} &= -(i\omega_b + \kappa_b)\delta b - \left(\frac{G_{+b}}{2}\delta A_+^\dagger + \frac{G_{-b}}{2}\delta A_-^\dagger - \text{H. c.}\right) + \sqrt{2\kappa_b}b^{in},\end{aligned}\quad (\text{B3})$$

where $\tilde{\Delta}_+ = \Delta_+ + 2G_0\text{Re}\langle b \rangle \sin^2\theta$ and $\tilde{\Delta}_- = \Delta_- + 2G_0\text{Re}\langle b \rangle \cos^2\theta$ are the effective polariton-drive detunings including the frequency shift caused by the dispersive coupling with the phonons. $G_{+b} \equiv G_{+-} \sin\theta$ ($G_{-b} \equiv G_{+-} \cos\theta$) represents the coupling strength between the polariton A_+ (A_-) and the phonon mode, where $G_{+-} \equiv G_+ \sin\theta + G_- \cos\theta$, with $G_\pm = i2G_0\langle A_\pm \rangle$ being the enhanced dispersive coupling strengths associated with the two CMPs.

The expressions of the steady-state averages are given by

$$\begin{aligned}\langle A_+ \rangle &= \frac{\Omega}{\mathcal{D}} \left[\delta\kappa \cos\theta - i \sin\theta (\tilde{\Delta}_- - 2G_0\text{Re}\langle b \rangle \cos^2\theta - i\kappa_-) \right], \\ \langle A_- \rangle &= \frac{\Omega}{\mathcal{D}} \left[\delta\kappa \sin\theta - i \cos\theta (\tilde{\Delta}_+ - 2G_0\text{Re}\langle b \rangle \sin^2\theta - i\kappa_+) \right], \\ \text{Re}\langle b \rangle &= -\frac{G_0}{\omega_b} \left[\langle A_+ \rangle \sin\theta + \langle A_- \rangle \cos\theta \right]^2,\end{aligned}\quad (\text{B4})$$

with $\mathcal{D} = -\mathcal{G}(\mathcal{G} - 2i\delta\kappa) + (\tilde{\Delta}_- - i\kappa_-)(\tilde{\Delta}_+ - i\kappa_+) + \delta\kappa^2$. The optimal condition for the polariton entanglement corresponds to $\tilde{\Delta}_+ = -\tilde{\Delta}_- \simeq \omega_b$, as discussed in the main text. Typically, the frequency shift due to the dispersive coupling is much smaller than the resonance frequency ω_b . Therefore, hereinafter we safely take $|\tilde{\Delta}_\pm| \simeq |\Delta_\pm| \simeq \omega_b$. This leads to the following simplified expressions

$$\langle A_+ \rangle \simeq \frac{\delta\kappa\Omega \cos\theta - i\Omega \sin\theta(\Delta_- - i\kappa_-)}{(\Delta_- - i\kappa_-)(\Delta_+ - i\kappa_+) + \delta\kappa^2}, \quad (\text{B5})$$

$$\langle A_- \rangle \simeq \frac{\delta\kappa\Omega \sin\theta - i\Omega \cos\theta(\Delta_+ - i\kappa_+)}{(\Delta_- - i\kappa_-)(\Delta_+ - i\kappa_+) + \delta\kappa^2}, \quad (\text{B6})$$

and the QLEs

$$\begin{aligned}\delta\dot{A}_+ &= -(i\Delta_+ + \kappa_+)\delta A_+ - \delta\kappa\delta A_- - G_{+b}\frac{\delta b + \delta b^\dagger}{2} + \sqrt{2\kappa_+}A_+^{in}, \\ \delta\dot{A}_- &= -(i\Delta_- + \kappa_-)\delta A_- - \delta\kappa\delta A_+ - G_{-b}\frac{\delta b + \delta b^\dagger}{2} + \sqrt{2\kappa_-}A_-^{in}, \\ \delta\dot{b} &= -(i\omega_b + \kappa_b)\delta b - \left(\frac{G_{+b}}{2}\delta A_+^\dagger + \frac{G_{-b}}{2}\delta A_-^\dagger - \text{H. c.}\right) + \sqrt{2\kappa_b}b^{in}.\end{aligned}\quad (\text{B7})$$

For simplicity, we neglect the *weak* coupling terms $\mathcal{G}(\delta A_+^\dagger \delta A_- + \delta A_+ \delta A_-^\dagger)$ between the two CMPs, which have a negligible impact on the entanglement. We, however, keep the coupling terms $-i\delta\kappa(\delta A_+^\dagger \delta A_- + \delta A_+ \delta A_-^\dagger)$, in order to study the impact of a possibly large $\delta\kappa$ of the system on the entanglement.

The QLEs (B7) can be expressed in the quadrature form, given by

$$\begin{aligned}\delta\dot{X}_+ &= \Delta_+\delta Y_+ - \kappa_+\delta X_+ - \delta\kappa\delta X_- - \text{Re}G_{+b}\delta X_b + \sqrt{2\kappa_+}X_+^{in}, \\ \delta\dot{Y}_+ &= -\Delta_+\delta X_+ - \kappa_+\delta Y_+ - \delta\kappa\delta Y_- - \text{Im}G_{+b}\delta X_b + \sqrt{2\kappa_+}Y_+^{in}, \\ \delta\dot{X}_- &= \Delta_-\delta Y_- - \kappa_-\delta X_- - \delta\kappa\delta X_+ - \text{Re}G_{-b}\delta X_b + \sqrt{2\kappa_-}X_-^{in}, \\ \delta\dot{Y}_- &= -\Delta_-\delta X_- - \kappa_-\delta Y_- - \delta\kappa\delta Y_+ - \text{Im}G_{-b}\delta X_b + \sqrt{2\kappa_-}Y_-^{in}, \\ \delta\dot{X}_b &= \omega_b\delta Y_b - \kappa_b\delta X_b + \sqrt{2\kappa_b}X_b^{in}, \\ \delta\dot{Y}_b &= -\omega_b\delta X_b - \kappa_b\delta Y_b - \text{Im}G_{+b}\delta X_+ + \text{Re}G_{+b}\delta Y_+ \\ &\quad - \text{Im}G_{-b}\delta X_- + \text{Re}G_{-b}\delta Y_- + \sqrt{2\kappa_b}Y_b^{in},\end{aligned}\quad (\text{B8})$$

where $\delta X_\pm = (\delta A_\pm + \delta A_\pm^\dagger)/\sqrt{2}$, $\delta Y_\pm = i(\delta A_\pm^\dagger - \delta A_\pm)/\sqrt{2}$, and $\delta X_b = (\delta b + \delta b^\dagger)/\sqrt{2}$, $\delta Y_b = i(\delta b^\dagger - \delta b)/\sqrt{2}$. The quadratures of the input noises X_j^{in} and Y_j^{in} ($j = +, -, b$) are defined in the same way. The above QLEs can be cast in the simple matrix form of

$$\dot{u}(t) = \mathcal{R}u(t) + n(t), \quad (\text{B9})$$

where $u(t) = [\delta X_+(t), \delta Y_+(t), \delta X_-(t), \delta Y_-(t), \delta X_b(t), \delta Y_b(t)]^T$, $n(t) = [\sqrt{2\kappa_+}X_+^{in}, \sqrt{2\kappa_+}Y_+^{in}, \sqrt{2\kappa_-}X_-^{in}, \sqrt{2\kappa_-}Y_-^{in}, \sqrt{2\kappa_b}X_b^{in}, \sqrt{2\kappa_b}Y_b^{in}]^T$, and the drift matrix \mathcal{R} is given by

$$\mathcal{R} = \begin{pmatrix} -\kappa_+ & \Delta_+ & -\delta\kappa & 0 & -\text{Re}G_{+b} & 0 \\ -\Delta_+ & -\kappa_+ & 0 & -\delta\kappa & -\text{Im}G_{+b} & 0 \\ -\delta\kappa & 0 & -\kappa_- & \Delta_- & -\text{Re}G_{-b} & 0 \\ 0 & -\delta\kappa & -\Delta_- & -\kappa_- & -\text{Im}G_{-b} & 0 \\ 0 & 0 & 0 & 0 & -\kappa_b & \omega_b \\ -\text{Im}G_{+b} & \text{Re}G_{+b} & -\text{Im}G_{-b} & \text{Re}G_{-b} & -\omega_b & -\kappa_b \end{pmatrix}. \quad (\text{B10})$$

[1] B. Z. Rameshti, S. V. Kusminskiy, J. A. Haigh, K. Usami, D. Lachance-Quirion, Y. Nakamura, C.-M. Hu, H. X. Tang, G. E.

W. Bauer, and Y. M. Blanter, Cavity magnonics, Phys. Rep.

- 979**, 1 (2022).
- [2] H. Huebl, C.W. Zollitsch, J. Lotze, F. Hocke, M. Greifenstein, A.Marx,R.Gross, and S. T. B.Goennenwein, High Cooperativity in Coupled Microwave Resonator Ferrimagnetic Insulator Hybrids, *Phys. Rev. Lett.* **111**, 127003 (2013).
 - [3] Y. Tabuchi, S. Ishino, T. Ishikawa, R. Yamazaki, K. Usami, and Y. Nakamura, Hybridizing Ferromagnetic Magnons and Microwave Photons in the Quantum Limit, *Phys. Rev. Lett.* **113**, 083603 (2014).
 - [4] X. Zhang, C. L. Zou, L. Jiang, and H. X. Tang, Strongly Coupled Magnons and Cavity Microwave Photons, *Phys. Rev. Lett.* **113**, 156401 (2014).
 - [5] Ö. O. Soykal and M. E. Flatté, Strong Field Interactions between a Nanomagnet and a Photonic Cavity, *Phys. Rev. Lett.* **104**, 077202 (2010).
 - [6] X. Zuo, Z.-Y. Fan, H. Qian, M.-S. Ding, H. Tan, H. Xiong, and J. Li, Cavity magnomechanics: from classical to quantum, *New J. Phys.* **26**, 031201 (2024).
 - [7] J. Li, S.-Y. Zhu, and G. S. Agarwal, Magnon-Photon-Phonon Entanglement in Cavity Magnomechanics, *Phys. Rev. Lett.* **121**, 203601 (2018).
 - [8] J. Li and S.-Y. Zhu, Entangling two magnon modes via magnetostrictive interaction, *New J. Phys.* **21**, 085001 (2019).
 - [9] Z. Zhang, M. O. Scully, and G. S. Agarwal, Quantum entanglement between two magnon modes via Kerr nonlinearity driven far from equilibrium, *Phys. Rev. Research* **1**, 023021 (2019).
 - [10] H. Tan, Genuine photon-magnon-phonon Einstein-Podolsky-Rosen steerable nonlocality in a continuously-monitored cavity magnomechanical system, *Phys. Rev. Research* **1**, 033161 (2019).
 - [11] H. Y. Yuan, S. Zheng, Z. Ficek, Q. Y. He, and M.-H. Yung, Enhancement of magnon-magnon entanglement inside a cavity, *Phys. Rev. B* **101**, 014419 (2020).
 - [12] H. Y. Yuan, P. Yan, S. Zheng, Q. Y. He, K. Xia, and M.-H. Yung, Steady Bell State Generation via Magnon-Photon Coupling, *Phys. Rev. Lett.* **124**, 053602 (2020).
 - [13] M. Yu, H. Shen, and J. Li, Magnetostrictively Induced Stationary Entanglement between Two Microwave Fields, *Phys. Rev. Lett.* **124**, 213604 (2020).
 - [14] M. Elyasi, Y. M. Blanter, and G. E. W. Bauer, Resources of nonlinear cavity magnonics for quantum information, *Phys. Rev. B* **101**, 054402 (2020).
 - [15] J. M. P. Nair and G. S. Agarwal, Quantum drives produce strong entanglement between YIG samples without using intrinsic nonlinearities, *Appl. Phys. Lett.* **117**, 084001 (2020).
 - [16] M. Yu, S.-Y. Zhu, and J. Li, Macroscopic entanglement of two magnon modes via quantum correlated microwave fields, *J. Phys. B* **53**, 065402 (2020).
 - [17] S.-S. Zheng, F.-X. Sun, H.-Y. Yuan, Z. Ficek, Q.-H. Gong, and Q.-Y. He, Enhanced entanglement and asymmetric EPR steering between magnons, *Sci. China-Phys. Mech. Astron.* **64**, 210311 (2021).
 - [18] D.-W. Luo, X.-F. Qian, and T. Yu, Nonlocal magnon entanglement generation in coupled hybrid cavity systems, *Opt. Lett.* **46**, 1073 (2021).
 - [19] J. Li and S. Gröblacher, Entangling the vibrational modes of two massive ferromagnetic spheres using cavity magnomechanics, *Quantum Sci. Technol.* **6**, 024005 (2021).
 - [20] Y.-T. Chen, L. Du, Y. Zhang, and J.-H. Wu, Perfect transfer of enhanced entanglement and asymmetric steering in a cavity-magnomechanical system, *Phys. Rev. A* **103**, 053712 (2021).
 - [21] D. Kong, X. Hu, L. Hu, and J. Xu, Magnon-atom interaction via dispersive cavities: Magnon entanglement, *Phys. Rev. B* **103**, 224416 (2021).
 - [22] W.-J. Wu, Y.-P. Wang, J.-Z. Wu, J. Li, and J. Q. You, Remote magnon entanglement between two massive ferrimagnetic spheres via cavity optomagnonics, *Phys. Rev. A* **104**, 023711 (2021).
 - [23] Z.-B. Yang, X.-D. Liu, X.-Y. Yin, Y. Ming, H.-Y. Liu, and R.-C. Yang, Controlling Stationary One-Way Quantum Steering in Cavity Magnonics, *Phys. Rev. Applied* **15**, 024042 (2021).
 - [24] V. A. Mousolou, Y. Liu, A. Bergman, A. Delin, O. Eriksson, M. Pereiro, D. Thonig, and E. Sjöqvist, Magnon-magnon entanglement and its quantification via a microwave cavity, *Phys. Rev. B* **104**, 224302 (2021).
 - [25] H. Xie, Z.-G. Shi, L.-W. He, X. Chen, C.-G. Liao, and X.-M. Lin, Proposal for a Bell test in cavity optomagnonics, *Phys. Rev. A* **105**, 023701 (2022).
 - [26] S.-F. Qi and J. Jing, Generation of Bell and GHZ states from a hybrid qubit-photon-magnon system, *Phys. Rev. A* **105**, 022624 (2022).
 - [27] Y.-L. Ren, J.-K. Xie, X.-K. Li, S.-L. Ma, and F.-L. Li, Long-range generation of a magnon-magnon entangled state, *Phys. Rev. B* **105**, 094422 (2022).
 - [28] B. Hussain, S. Qamar, and M. Irfan, Entanglement enhancement in cavity magnomechanics by an optical parametric amplifier, *Phys. Rev. A* **105**, 063704 (2022).
 - [29] W. Qiu, X. Cheng, A. Chen, Y. Lan, and W. Nie, Controlling quantum coherence and entanglement in cavity magnomechanical systems, *Phys. Rev. A* **105**, 063718 (2022).
 - [30] Y. Zhou, S. Y. Xie, C. J. Zhu, and Y. P. Yang, Nonlinear pumping induced multipartite entanglement in a hybrid magnon cavity QED system, *Phys. Rev. B* **106**, 224404 (2022).
 - [31] Z.-Y. Fan, H. Qian, and J. Li, Stationary optomagnonic entanglement and magnon-to-optics quantum state transfer via optomagnomechanics, *Quantum Sci. Technol.* **8**, 015014 (2023).
 - [32] H. Qian, Z.-Y. Fan, and J. Li, Entangling mechanical vibrations of two massive ferrimagnets by fully exploiting the nonlinearity of magnetostriction, *Quantum Sci. Technol.* **8**, 015022 (2023).
 - [33] Z.-Y. Fan, H. Qian, X. Zuo, and J. Li, Entangling ferrimagnetic magnons with an atomic ensemble via optomagnomechanics, *Phys. Rev. A* **108**, 023501 (2023).
 - [34] J. Chen, X.-G. Fan, W. Xiong, D. Wang, and L. Ye, Nonreciprocal entanglement in cavity-magnon optomechanics, *Phys. Rev. B* **108**, 024105 (2023).
 - [35] Z.-Y. Fan, L. Qiu, S. Gröblacher, and J. Li, Microwave-optics Entanglement via Cavity Optomagnomechanics, *Laser Photonics Rev.* **17**, 2200866 (2023).
 - [36] J. Xie, H. Yuan, S. Ma, S. Gao, F. Li, and R. A. Duine, Stationary quantum entanglement and steering between two distant macromagnets, *Quantum Sci. Technol.* **8**, 035022 (2023).
 - [37] C.-J. Yang, Q. Tong, and J.-H. An, Quantum-state engineering in cavity magnomechanics formed by two-dimensional magnetic materials, *New J. Phys.* **26**, 023032 (2024).
 - [38] N. Hu and H. Tan, Two-tone modulated cavity electromagnonics, arXiv:2305.10653.
 - [39] C. W. Gardiner and P. Zoller, *Quantum Noise* (Springer, Berlin, 2000).
 - [40] D. Vitali, S. Gigan, A. Ferreira, H. R. Böhm, P. Tombesi, A. Guerreiro, V. Vedral, A. Zeilinger, and M. Aspelmeyer, Optomechanical Entanglement between a Movable Mirror and a Cavity Field, *Phys. Rev. Lett.* **98**, 030405 (2007).
 - [41] X. Zhang, C.-L. Zou, L. Jiang, and H. X. Tang, Cavity magnomechanics, *Sci. Adv.* **2**, e1501286 (2016).
 - [42] C. A. Potts, E. Varga, V. Bittencourt, S. V. Kusminskiy, and J. P. Davis, Dynamical Backaction Magnomechanics, *Phys. Rev. X* **11**, 031053 (2021).
 - [43] R.-C. Shen, J. Li, Z.-Y. Fan, Y.-P. Wang, and J. Q. You, Me-

- chanical Bistability in Kerr-modified Cavity Magnomechanics, *Phys. Rev. Lett.* **129**, 123601 (2022).
- [44] G. Vidal and R. F. Werner, Computable measure of entanglement, *Phys. Rev. A* **65**, 032314 (2002).
- [45] G. Adesso, A. Serafini, and F. Illuminati, Extremal entanglement and mixedness in continuous variable systems, *Phys. Rev. A* **70**, 022318 (2004).
- [46] M. B. Plenio, Logarithmic Negativity: A Full Entanglement Monotone That is not Convex, *Phys. Rev. Lett.* **95**, 090503 (2005).
- [47] J. Li, I. M. Haghghi, N. Malossi, S. Zippilli, and D. Vitali, Generation and detection of large and robust entanglement between two different mechanical resonators in cavity optomechanics, *New J. Phys.* **17**, 103037 (2015).
- [48] S. G. Hofer, W. Wieczorek, M. Aspelmeyer, and K. Hammerer, Quantum entanglement and teleportation in pulsed cavity optomechanics, *Phys. Rev. A* **84**, 052327 (2011).
- [49] G. Flower, J. Bourhill, M. Goryachev, and M. E. Tobar, Broadening frequency range of a ferromagnetic axion haloscope with strongly coupled cavity-magnon polaritons, *Physics of the Dark Universe* **25**, 100306 (2019).
- [50] N. Crescini, D. Alesini, C. Braggio, G. Carugno, D. D'Agostino, D. Di Gioacchino, P. Falferi, U. Gambardella, C. Gatti, G. Iannone, C. Ligi, A. Lombardi, A. Ortolan, R. Pengo, G. Ruoso, and L. Taffarello (QUAX Collaboration), Axion Search with a Quantum-Limited Ferromagnetic Haloscope, *Phys. Rev. Lett.* **124**, 171801 (2020).
- [51] S. Chigusa, T. Moroi, and K. Nakayama, Detecting light boson dark matter through conversion into a magnon, *Phys. Rev. D* **101**, 096013 (2020).
- [52] V. Giovannetti, S. Lloyd, and L. Maccone, Advances in quantum metrology, *Nat. Photon.* **5**, 222 (2011).
- [53] Y. Xia, A. R. Agrawal, C. M. Pluchar, A. J. Brady, Z. Liu, Q. Zhuang, D. J. Wilson, and Z. Zhang, Entanglement-enhanced optomechanical sensing, *Nat. Photon.* **17**, 470 (2023).
- [54] C. Ciuti, Branch-entangled polariton pairs in planar microcavities and photonic wires, *Phys. Rev. B* **69**, 245304 (2004).